Hindawi
Shock and Vibration
Volume 2023, Article ID 2145765, 14 pages
https://doi.org/10.1155/2023/2145765

Research Article

Unified Mechanism of Rock Burst Induced by Coal Mine Earthquake and Its Activity and Response Characteristics

Pengfei Lyu and Yijian Geng

School of Mining and Coal Engineering, Inner Mongolia University of Science and Technology, Inner Mongolia Baotou 014000, China

Correspondence should be addressed to Pengfei Lyu; 2018930@imust.edu.cn

Received 26 September 2022; Revised 30 October 2022; Accepted 24 November 2022; Published 14 February 2023

Academic Editor: Leibo Song

The occurrence regularity of the coal mine earthquake under the influence of hard roof, fault, and mining was studied by theoretical analysis, field investigation, and monitoring data analysis for the phenomenon of rock burst induced by coal mine earthquakes. The dissipation characteristics of coal mine earthquake energy propagation considering a hypocenter scale were described, and the coal mine earthquake response characteristics were analyzed. The two principles of rock burst induced by hard rock fractured type coal mine earthquakes and the three principle of rock burst induced by fault were described. Based on this, the unified mechanism rock burst induced by different types of coal mine earthquakes was proposed. The results show that the microseismic energy increases sharply and decreases sharply when mining in the fault area. The amplitude and frequency of support resistance increased before and after the heavy coal mine earthquake occurred. The periodic characteristics of the coal mine earthquake in the 43_{upper} 13 working face of the Dongtan coal mine show that there are 50 m small periods within 100 m large periods. The multiparameter field monitoring can make it possible for instantaneous capture of the coal mine earthquake dynamic responses. The unified rock burst mechanism induced different types of coal mine earthquake and is the difference energy between the superposition energy of the rock burst source region and the energy consumed by coal-rock instability increases suddenly under the action of coal mine earthquakes. Meanwhile, the violent rock burst accident occurs when the stiffness condition is satisfied.

1. Introduction

The coal mine earthquake and rock burst are the main dynamic disasters in coal mining. But they are different and connected. The coal mine earthquake is a microearthquake induced by mining. The coal mine earthquake has little effect on safety mining when below level 3.0. The rock burst is a dynamic phenomenon that the stress overrun near the mining face or roadway is excited by the instantaneous throw of coal-rock mass, which will cause certain damage to underground equipment and workers [1, 2]. The coal-rock impact instability was usually caused by the superposition of coal mine earthquake energy and static load energy near the mining face. At the same time, the coal-rock impact on surrounding rock is also a strong dynamic disturbance and it may induce a strong coal mine earthquake. Therefore, in order to realize the safety mining, it is of great significance to study on the regularity and mechanism of rock burst induced by the coal mine earthquake in the coal mining face.

The coal mine earthquake is a kind of induced microearthquake and its occurrence is usually random. In recent years, the microseismic monitoring equipment has been put into coal mining which provides great convenience for the study of coal mine earthquake characteristics. The coal mine earthquake characteristics have gradually become clear and credible from the original random. They studied the coal mine earthquake activity law of deep stress concentration area, high constructed stress area, and hard roof reserve area by the microseismic monitoring system in references [3–7]. They believed that the occurrence of strong coal mine earthquakes was usually correlated positively with the maximum vertical stress gradient. Most of the syncline axes were near the geological structures and adjacent fault zones. Its strength was obviously affected by mining speed and roof weighting. The theoretical analysis and numerical simulation were used to study the spatial and temporal characteristics of strong coal mine earthquake rock burst induced by overburden movement in references [8, 9]. The breaking of the main key stratum which determines the motion mode of the inferior key stratum was considered. They combined the motion of the inferior key strata before the main key strata break. It accompanied the frequent occurrence of the low-energy coal mine earthquake. The earthquake hypocenter spread throughout the working face and the strong coal mine earthquake frequently occurs after the primary break off a main key stratum. The earthquake hypocenter plane was transverse *O-X* distribution. The quantitative relationship between mining activities and coal mine earthquakes was discussed under the microseismic and mining data in references [10, 11]. It was considered that continuous mining has a cumulative effect on strong coal mine earthquake occurrence. Adjusting the operation flow is an effective way to reduce coal mine earthquake disasters. The attenuation law of coal mine earthquake vibration wave by the underground blasting test was analyzed in references [12, 13]. And the concussion energy and the main frequency showed a power exponential attenuation change.

The study on the mechanism of coal mine earthquake rock burst induced mainly focuses on the fault-type coal mine earthquake and hard roof type coal mine earthquake. Taking the normal fault as an example in references [14, 15], the influence of fault activity on rock burst was analyzed. It was considered that the influence of fault on rock burst was reflected in changing the physical mechanical properties and the original structure stress field of coal-rock near the fault. The sensitive index of the fault slip instability rock burst induced was based on the Yima F16 fault in references [16, 17]. So, the relation model between the stress field and impact strength in the fault zone was established. The effect of different dip angles of reverse faults on rock burst was analyzed in references [18, 19]. The stress of the fault upper plate increases with the increase of fault dip angle when the inclination angle is less than 45°. The lower plate of the fault was the opposite. The evolution process of the stress field near normal fault by numerical simulation was analyzed in references [20, 21]. It was considered that the high stress in "inverted wedge" area between the working face and fault when the upper plate was mining towards the fault. It is a rock burst in multiple areas.

It mainly studied about the hard roof type coal mine earthquake in references [22–29]. The large overburden area easily produced a strong dynamic load and induced rock burst after breaking hard roof in references [22, 23]. The occurrence mechanism of rock burst under the control of thick conglomerate and thrust fault was analyzed in references [24, 25]. The superposition sum of the transmissible stress of thick conglomerate and construction stress of thrust fault was estimated. The stress and overrun are the fundamental causes of rock burst. The impact instability process of the hard roof adjacent to the coal pillar and carrying out mechanical calculation was analyzed in references [26, 27]. It was considered that the instability the of adjacent coal pillar was seriously affected by the periodic weighting of a hard roof. The hard roof must be controlled in advance for the treatment of rock burst induced by mine earthquakes in references [28, 29]. It can adopt measures such as pre-splitting the roof and cutting roof hung up. The disaster management process is as follows: cause analysis $\longrightarrow$ Roof pressure relief $\longrightarrow$ Effect testing $\longrightarrow$ Safe mining.

The above studies are related to the occurrence regularity of coal mine earthquakes and the mechanism of rock burst induced by different conditions. But there are few studies on coal mine earthquake response characteristics. They were studied relatively independently. It lacks the study of the corresponding rock burst-induced mechanism for various types of rock burst. The author embarks from coal mine earthquake occurrence rule angle. It analyzed the coal mine earthquake characteristics of the hard roof and fault zone. The influence of mining factors of coal mine earthquake is also analyzed. Second, the propagation and dissipation characteristics of the coal mine earthquake energy were studied. The response characteristics of the coal mine earthquake are based on field monitoring. At last, the principle of strong coal mine earthquake induced by hard roof and fault activation was described. The unified-induced mechanism of different types of strong coal mine earthquakes rock burst induced by differential energy sharp increase was proposed. The research conclusion aims to make the research on the occurrence and induction of coal mine earthquake more systematic and relevant and then guide the engineering practice.

2. Correlation Analysis of Coal Mine Earthquake Activity Law

2.1. Relationship between Hard Roof and Occurrence of Coal Mine Earthquakes. Many high-energy coal mine earthquakes have occurred in the 43_{upper} 13 working face of Dongtan coal mine, and they may have some relationship with the hard roof. Therefore, the drillhole data were analyzed which included 6–2 drillhole, J 9–3 drillhole, and B 7 drillhole, as shown in Figure 1. The 6–2 borehole columnar section (Figure 1(a)) shows that immediate roof and immediate floor of 3_{upper} coal seam are thick mudstones. The mudstone has a great blocking effect on stress wave transmission. So, there are less coal mine earthquakes in the initial mining stage and they have lower energy. The J 3–9 borehole columnar section (Figure 1(b)) shows that immediate roof and immediate floor are hard siltstones which may be induced by a certain level of coal mine earthquake. The B 7 borehole columnar section (Figure 1(c)) shows that the roof of 3_{upper} coal seam is siltstone and medium sandstone with the height of 29.5 m. In summary, the roof is soft in the 43_{upper} 13 working face. The roof gradually hardens as the working face advances. The medium-fine sandstone of 3_{upper} above the coal seam with the average thickness is 14.7 m, and the strong pressure was caused by its fracture in working face. But according to the energy level, they may have rock

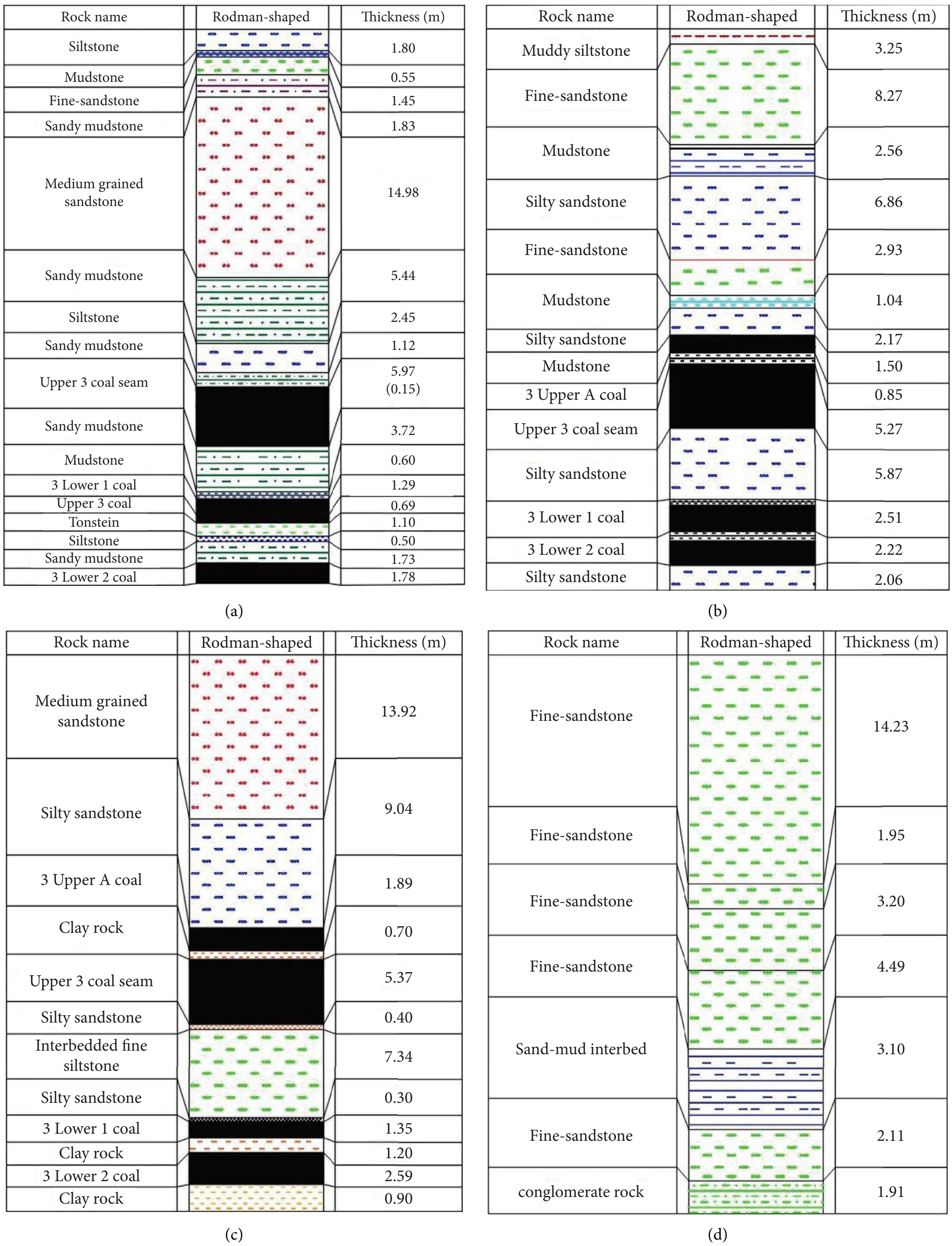

Figure 1: Coal seam columnar section. (a) J 6-2. (b) J 9-3. (c) B 7. (d) B 7 drillhole in a higher level.

burst induced above level 2.0 coal mine earthquake. So, the high level drillhole continuing was detected. Above the B 7 drillhole in high level with the height is 86 m, and there are sandy conglomerates with the thickness of 37 m (Figure 2(d)). Many high-energy coal mine earthquakes have rock burst induced when the sand-conglomerate fractured. So, it is considered that the hard-thick sand-conglomerate above the 3_{upper} coal seam with the height is 90 m. It is the

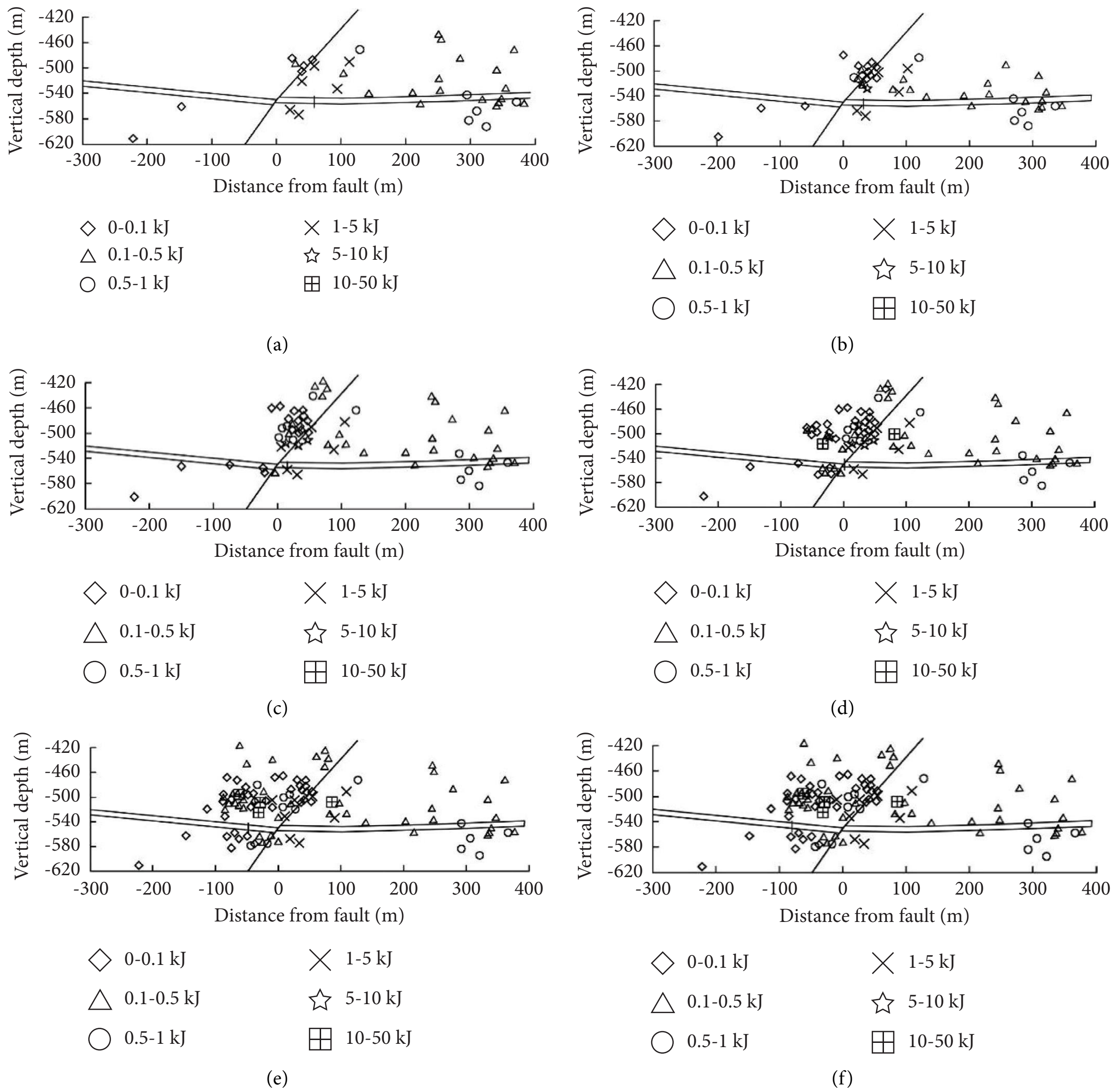

Figure 2: Seismic origin when caving pass through fault. (a) Distance of fault to working face is 62 m on July 26th. (b) Distance of fault to working face is 39 m on August 1st. (c) Distance of fault to working face is 18 m on August 6th. (d) Distance of fault to working face is 0 m on August 11th. (e) Distance of fault passing through the working face is 47 m on August 17th. (f) Distance of fault passing through the working face is 80 m on August 25th.

key rock strata and many high-energy coal mine earthquakes were induced in the working face. To achieve safe mining, there should be pressure relief of high hard-thick sandy conglomerates at first. The suggested measures of deep hole presplitting blasting and large diameter long hole pressure relief were adopted.

2.2. Coal Mine Earthquake Law in the Fault Zone

2.2.1. Distribution Characteristics of Mining Hypocenter in the Fault Zone. The middle of 14310 working face in the Dongtan coal mine was traversed by a normal fault which called NF 6. The fault of average drop is 3.1 m, and the average angle is 65°. The strong rock pressure was within 150 m near fault during mining, so the microseismic system was used for real-time monitoring while working face mining traversed the faults. The distribution of microseismic hypocenter of the working face mining approached and traversed the fault is as shown in Figure 2.

There were no microseismic events near the fault when the working face is far from the fault. It shows that the mining at this time has little effect for the fault and microseismic distribution remains the traditional regularity. Most of the hypocenter distributions were located in front of the coal rib and near the gob. There were sporadic microseismic events occurred near the fault when the working face advanced to 150 m from the fault. That means the fault was already activated. The number of microseismic events near the fault continued to increase continuously. But increase the rate was steady basically. The fault was activated continuously during this period. In fact, many horizontal stresses were accumulated in the upper and lower plates in the process of forming faults. The horizontal stress release and transfer was caused by fault activation. The fault activated rock bursts occurred near faults. On July 26th, the microseismic frequency suddenly increased when the distance from the coal rib to the fault was 62 m (Figure 2(a)). It shows that fault activation intensifies. The yield failure and fissure development of coal were affected by mining. The faults activation type rock burst was induced and should be released in advance. On August 1st, the high-energy microseismic events occurred (Figure 2(b)) when the distance from the coal rib to the fault was 39 m. The roof of continuity may have cut off by coal mining and the high-stress coal pillars were formed in a fault lower plate. The rock pressures were very strong under the dual role of the fault activation and the fault coal pillar. The fault coal pillar of rock burst has occurred easily. On August 6th, the high-energy microseismic frequently occurred when the distance from the coal rib to the fault was 18 m. The hypocenter largely focuses on the near the main roof of the fault (Figure 2(c)). It shows that the coal pillar stress has very high focus at this time. The fault is easily staggered between the upper plate and lower plate. The fault dislocation type rock bursts were induced. On August 11th, the mining of the fault traversed the working face (Figure 2(d)). At this time, the surrounding rock near the fault was seriously broken. The fault mud gushes out on the fault surface and the working environment of the mining face was bad. The large area connected support measures have been recommended to adopt. The fault lower plate mining was completed at this time. The upper fault mining began on August 12th. The distance of fault passing through the working face was 48 m on August 17th (Figure 2(e)). At this time, the high-energy microseisms still occurred. It was caused by the fault activation residual stress. The mining face still has a great risk of rock burst and the fault stress should be continuously released. On August 25th, the working face passing through the fault is 80 m (Figure 2(f)). The frequency of microseismic decreases and the high-energy microseismic no longer occurs. The hypocenter position again conforms to the traditional law. It indicated that the mining of working face is no longer affected by fault at this time.

2.2.2. Characteristics of the Microseismic Frequency and Energy Variation in the Fault Zone Mining. The statistics of microseismic frequency and energy during mining across fault in the 14310 working face are as shown in Figure 3. It can be seen that the fault activation was intensified, the frequency of microseismic events was increased sharply, and the microseismic energy was also increased since July 26th. However, the magnitude is not large and low-energy microseismic events remain dominant. The fault activation and fault coal pillar enter the dual action period on August 6th. The high-energy microseismic events occurred frequently and microseismic energy fluctuated. It shows two main laws. First, the microseismic energy always fluctuates at a certain level under normal conditions. But the microseismic energy change in this period was extremely unstable. The energy value increases sharply and decreases sharply and the energy amplitude gap increases. Second, before that, the high-energy events occurred. The microseismic frequency and energy have a downward trend. Later, the high-energy events occurred and then changed into low-energy and low-frequency law. It indicates that low-energy microseismic events have an action of energy storage for a high-energy microseismic event.

2.3. Relationship between Support Resistance and Coal Mine Earthquake. Taking coal mine earthquake events above level 2.0 in the 43_{upper} 13 working face of the Dongtan coal mine as an example, the relationship between high-energy coal mine earthquakes and support resistance was analyzed, as shown in Figure 4. The following characteristics are shown in Figures 4(a) and 4(b). The high-energy coal mine earthquake often occurs when the support resistances are longer than the safety valve opening value in two consecutive times. And the two events are 12–36 hours apart. The occurrence of large energy coal mine earthquakes was often continued, as shown in Figures 4(c) and 4(d). The second coal mine earthquake of similar magnitude occurs within 24 hours of a large coal mine earthquake. The following rules were found by observing the resistance curve of support: first, the support resistances are unsteady, the amplitude increases, and the frequency increases before the coal mine earthquakes. Second, the strong coal mine earthquakes often occur in the late stage of the support resistance increase period. So, there is a period of energy storage period before a strong coal mine earthquake occurs. Besides, the coal mine earthquake events of the 43_{upper} 13 working face above level 2.0 are all in or before the increase of support resistance in the working face. The times of elevated support resistance are 22 and it is accounting for 84.6%.

2.4. Relationship between Mining Speed and Occurrence of Coal Mine Earthquake. The daily propulsion curves of 43_{upper} 13 working face in the Dongtan coal mine from August 20th to October 10th is as shown in Figure 5. The occurrences of the strong coal mine earthquake mainly display as follows. First, before the two coal mine earthquakes on August 30th, the working face stopped mining for a period of time and then the mining speed increased rapidly. Before the coal mine earthquake on September 7th, mining speed decreased rapidly and fluctuated greatly. The mining speed continued to rise and the roof concussion occurred frequently before the coal mine earthquake on September 23th. The mining speed suddenly rises after a decline before the coal mine earthquake on October 6th. So, it is considered that the mining velocity concussion to some extent can promote the occurrence of large energy coal mine earthquakes. The mining speed should be increased slowly when mining again after stopping mining. The mining speed should be slowed down uniformly and kept stable when they meet the faults in mining. In addition, the overall mining of the working face should be kept as uniform velocity as possible. The sharp increase and decrease of the working face stress caused by the dramatic change of the mining speed were avoided.

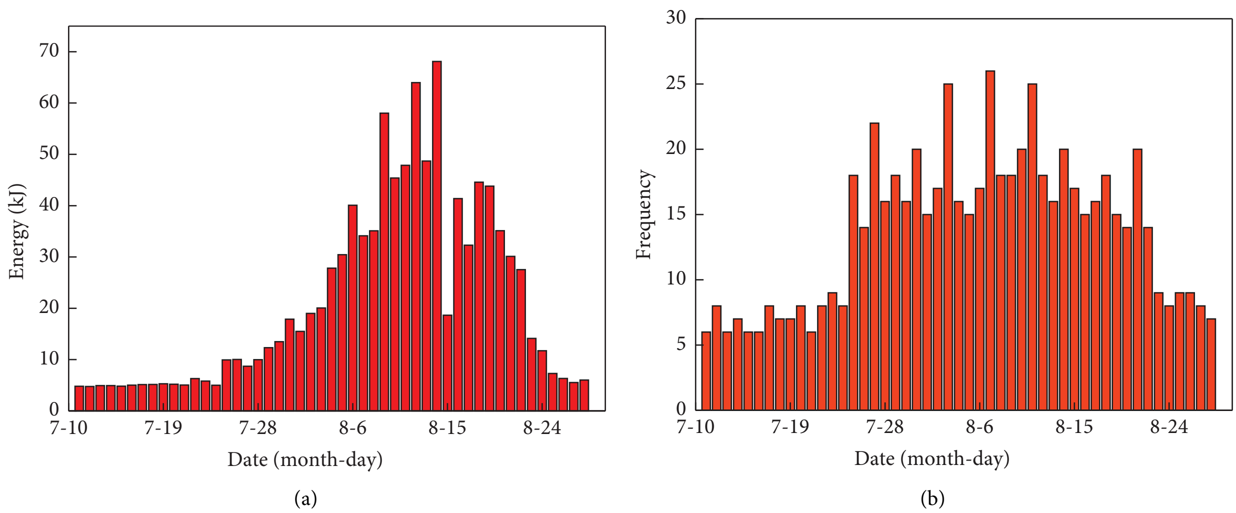

Figure 3: Energy and frequency change of caving when passing through fault. (a) Energy. (b) Frequency.

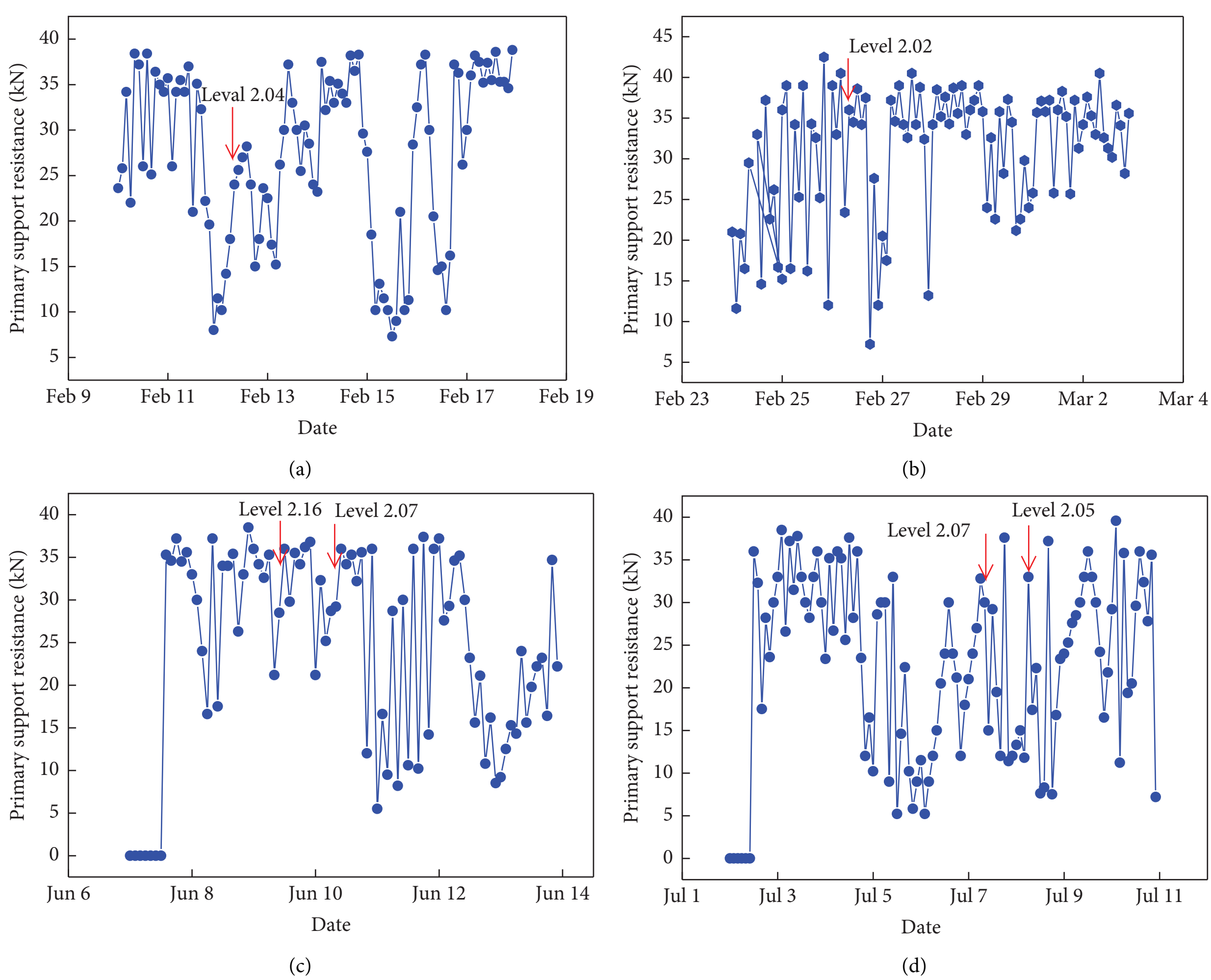

Figure 4: Support resistance before or after coal mine earthquakes. (a) February 12th. (b) February 26th. (c) June 9th and June 10th. (d) July 7th and July 8th.

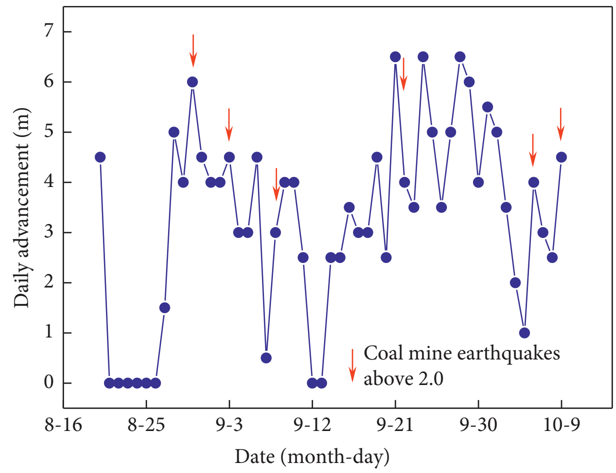

Figure 5: Relationship between coal mine earthquake and daily advancement.

2.5. Relationship between Working Face Footage and Occurrence of Coal Mine Earthquake. The study of seismology shows that the occurrence time and location of earthquake have periodicity, and the coal mine earthquakes are the same. The authors study the characteristics of coal mining earthquakes period from the angle of mining footage. Take 43_{upper} 13 working face of the Dongtan coal mine as an example. The statistics began from the position of working face mining to 31 m. First of all, let us take 100 meters as a period, and the occurrence times of the strong coal mine earthquakes in each mining cycle were counted. Then, take 50 m as a period. Count again the number of the strong coal mine earthquakes in each period. Narrow the period range again and statistic the period. The statistical results of time domain location of large energy coal mine earthquakes are shown in Table 1. According to the statistical results, the periodic characteristics of large energy coal mine earthquakes have considered and show there is the small period of 50 m within the large period of 100 m. There are 4 strong coalmine earthquakes in a large period and about 2 strong coal mine earthquakes in a small period. The observation results of rock pressure were combined, and the large and small periodic corresponding to the pressure of six and three main roof periodic were considered.

3. Propagation Law of Coal Mine Earthquake Energy and Response Characteristics of Coal-Rock Mass

3.1. Propagation Law of Coal Mine Earthquake Energy. The propagation of coal mine earthquake waves in rock mass is a nonlinear process. The propagation effect was related to the range of hypocenter area, the degree of fracture, and the microcosmic structure. For improving the traditional formula, the above factors were considered. The new formula of coal mine earthquake energy propagation dissipation with the hypocenter region r_0 was obtained as follows.

$$\begin{cases} E_{iP} = E_{0P} r_0^2 r_i^{-2} e^{-\left(2\pi f / v_P Q_P\right)\left(r_i - r_0\right)} \left(R^P\right)^2 \left(M_{ij}\right), \\ E_{iS} = E_{0S} r_0^2 r_i^{-2} e^{-\left(2\pi f / v_S Q_S\right)\left(r_i - r_0\right)} \left[\left(R^{SV}\right)^2 + \left(R^{SH}\right)^2\right] \left(M_{ij}\right), \\ E_i = E_{iP} + E_{iS}, \\ r_i \geq r_0, \mathrm{r}_0 \geq 1. \end{cases} \quad (1)$$

In the formula, E is the earthquake energy. The subscripts P and S are the P waves and S waves. r_i is the propagation distance of coal mine earthquake wave. f is the main frequency of coal mine earthquake waves. v_P and v_S are the P and S wave velocities. Q_P and Q_S are the dissipative quality factors of P and S wave propagation. R^P, R^{SV}, and R^{SH} represent the radiation mode of the coal mine earthquake wave. M_{ij} is the moment tensor of the hypocenter region. r_0 is the hypocenter region.

If the coal mine earthquake releases energy $E_{0P} = 500$ kJ and $E_{0S} = 500$ kJ, the vibration frequency $f = 8.15$ Hz, P wave velocity $= v_P = 3500$ m/s, S wave velocity $= v_S = 2000$ m/s, P wave dissipation quality factor $Q_P = 135$, S wave dissipation quality factor $Q_S = 95$, $(R^P)^2 = 1$, and $(R^{SV})^2 + (R^{SH})^2 = 1$. The seismic moment $M_{ij} = 1$. $r_0 = 1$, 10, 20, 40, and 60 m. The dissipation characteristics of the coal mine earthquake energy propagation described by formula (1) are shown in Figure 6. The faster is the propagation and dissipation rate of

Table 1: Relationship between the working face footage and coal mine earthquake.

Date	Footage on the day of mining earthquake (m)	Accumulative footage (m)	Footage range (m)	Footage period (m)
2015.2.12	6.75	115.3	31–131	100
2015.2.26	7.35	179.9		
2015.3.4	5.65	214	131–231	100
2015.3.5	6.25	220.3		
2015.3.30	1.45	299.3	231–331	100
2015.5.2	4.75	371.4		
2015.5.8	4.5	379.5		
2015.5.21	2.25	400.5	331–431	100
2015.5.26	3.75	412		
2015.6.9	3.5	423.5		
2015.6.10	6	429.5		
2015.6.14	4	445	431–481	50
2015.6.21	1.8	457.9		
2015.7.7	1.25	484.3		
2015.7.8	2.75	487	481–531	50
2015.7.14	3.25	503.8		
2015.7.25	3.5	542	531–581	50
2015.7.27	5	554.3		
2015.8.27	1.5	661.5	631–681	50
2015.8.30	6	676.5		
2015.9.03	4.5	693.7	681–731	50
2015.9.07	0.5	704.5		
2015.9.23	3.5	753.5	731–781	50
2015.10.06	4	811.3	781–831	50
2015.10.09	4.5	821.8		

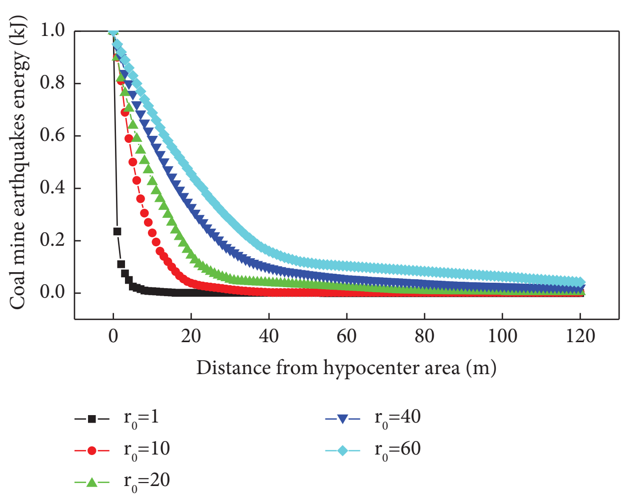

Figure 6: Dissipation characteristics of coal mine earthquakes energy propagation.

coal mine earthquake energy when the hypocenter area scale becomes smaller. The increase of the hypocenter area scale can slow down the magnitude of coal mine earthquake energy dissipation when the same coal mine earthquake energy was released.

What needs special explanation are the characteristics of coal mine earthquakes energy dissipation described, which are only qualitative descriptions of laws, as shown in Figure 6. The formula (1) was used to accurately calculate the coal mine earthquakes at a certain position. And more field tests are needed to accurately determine the parameters in formula (1).

3.2. Monitoring and Analysis of Coal Mine Earthquake Response Characteristics. The equipment are coal-rock stress meter, roof separation meter, and bolt stress meter. It can monitor the stress and displacement of coal body, roof displacement, and bolt force change in the process of coal mine earthquake. The response curve of each parameter when the coal mine earthquakes occur is shown in Figure 7. The distance of monitoring equipment to the hypocenter area is 176 m, 142 m, 208 m, and 194 m, respectively, as shown in Figures 7(a)–7(d).

It can be seen that the occurrence of coal mine earthquake forced the stress of coal body to decrease by 0.9 MPa instantly. The coal seam displacement change located in 8 mm. The maximum displacement of coal seam is 15 mm. And the roof separation shown by separator is finally 17 mm. The maximum separation is 28 mm. And the stress of bolt decreases by 9.1 kN. It shows that the vibration response causes the bolt loose. Even it has the possibility of failure. The field feedback has an obvious seismic response and the whole response time was 4–6 min.

The dynamic effect of stope, roadway, roof, and floor was caused by the coal mine earthquake. But the different vibration effects vary greatly. The multiparameter field monitoring can capture transient characteristics of coal mine earthquake response. The general location of the coal mine earthquake hypocenter can be judged according to the geological environment characteristics of the coal mine earthquake area. It can also be used to evaluate the degree of disaster caused by the coal mine earthquake.

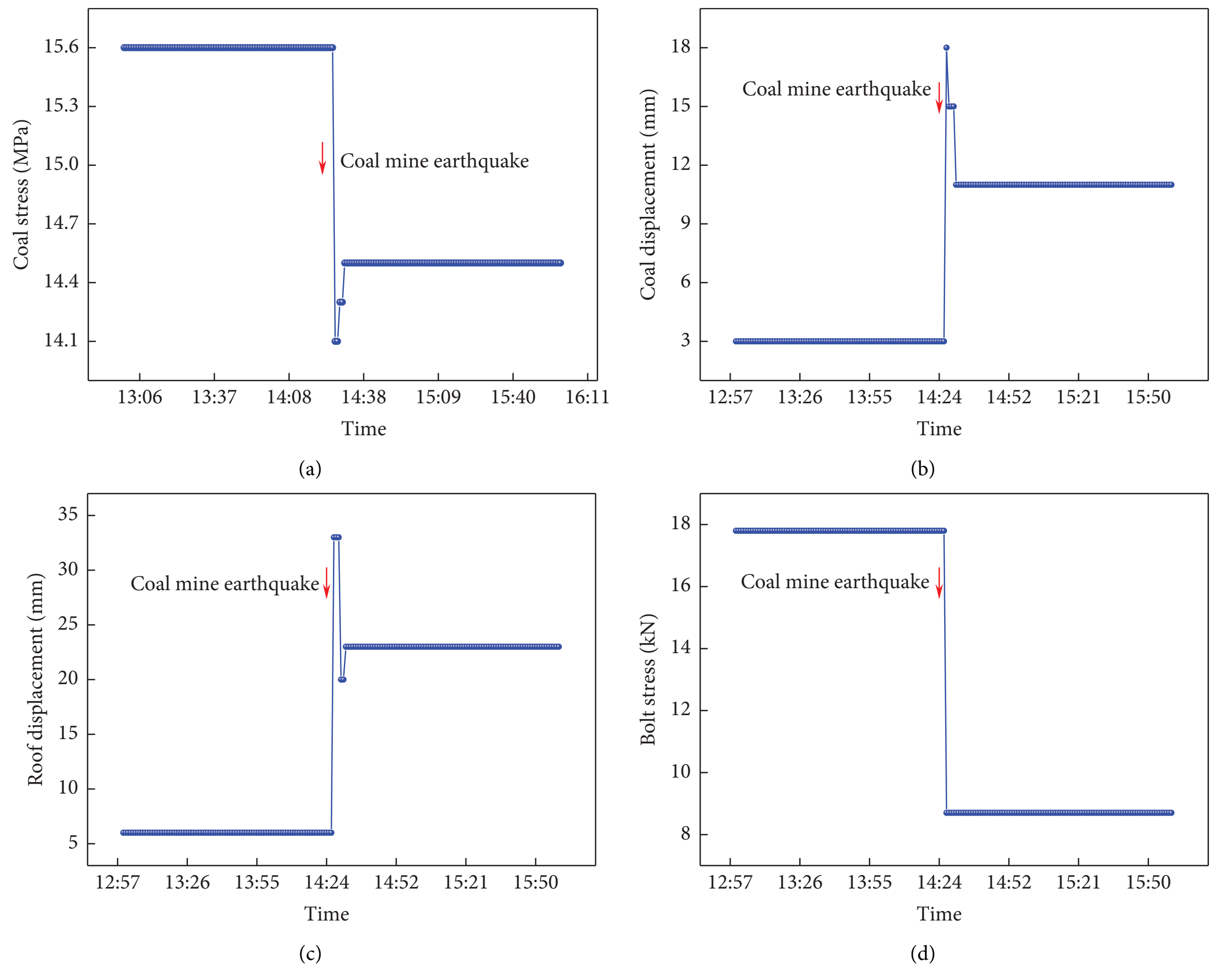

Figure 7: Parametric response curves during the coal mine earthquake. (a) Stress response curve of coal seam. (b) Displacement response curve of coal seam. (c) Roof displacement response curve. (d) Stress response curve of bolt.

4. Study on Mechanism of Rock Burst Induced by Coal Mine Earthquake

4.1. Rock Burst-Induced Principle of Hard Rock Fracture Type Coal Mine Earthquake. According to the coal mine earthquake law, under the condition of roof hard rock, distribution and movement characteristics of hard rock can be known. The occurrence of rock burst under the influence of roof hard rock can be divided into two types: hard rock shear fracture-induced rock burst and hard rock sliding settlement-induced rock burst. The following are described, respectively, in Figure 8.

4.1.1. Rock Burst-Induced Principle of Hard Rock Shear Breaking. The overlying rock structure was disturbed by working face mining or roadway excavating. The roof of coal seam collapses or breaks under normal circumstances and it forms the hinged rock blocks. Its mechanical properties make its rupture period longer than other rock strata when the roof reserved the hard-thick rock strata. Additional thickness increases and the elastic energy accumulation of rock strata. The large energy was released by breaking. The breaking released energy was transferred to the vicinity of the coal rib and superimposed with the mining static load energy. The impact appears in the coal rib near the working face or roadway, as shown in Figure 8(a). Rock block A and rock block B will form large energy coal mine earthquakes in fault subsidence. The shock appearances of coal rib near the gob were induced.

4.1.2. Rock Burst-Induced Principle of Impulse Hard Rock Sliding Settlement. The large energy coal mine earthquakes were not formed with the fault of rock blocks A and rock blocks B sunk. There is another situation that may induce rock burst. The subsidence increases and separates from the upper strata when rock block A and rock block B were sunk. The stress was concentrated near blocks A and B at the top of rock block C and rock block D. The trend of rock block C and rock block D inclined downward, slip dislocation increases and the subsidence of rock block A and rock block B increases. It may cause instantaneous slide of hard rock block C and rock block D to form a large dynamic load. The static load superposition may induce rock burst when it passes to the adjacent coal rib. In addition, it can be seen that

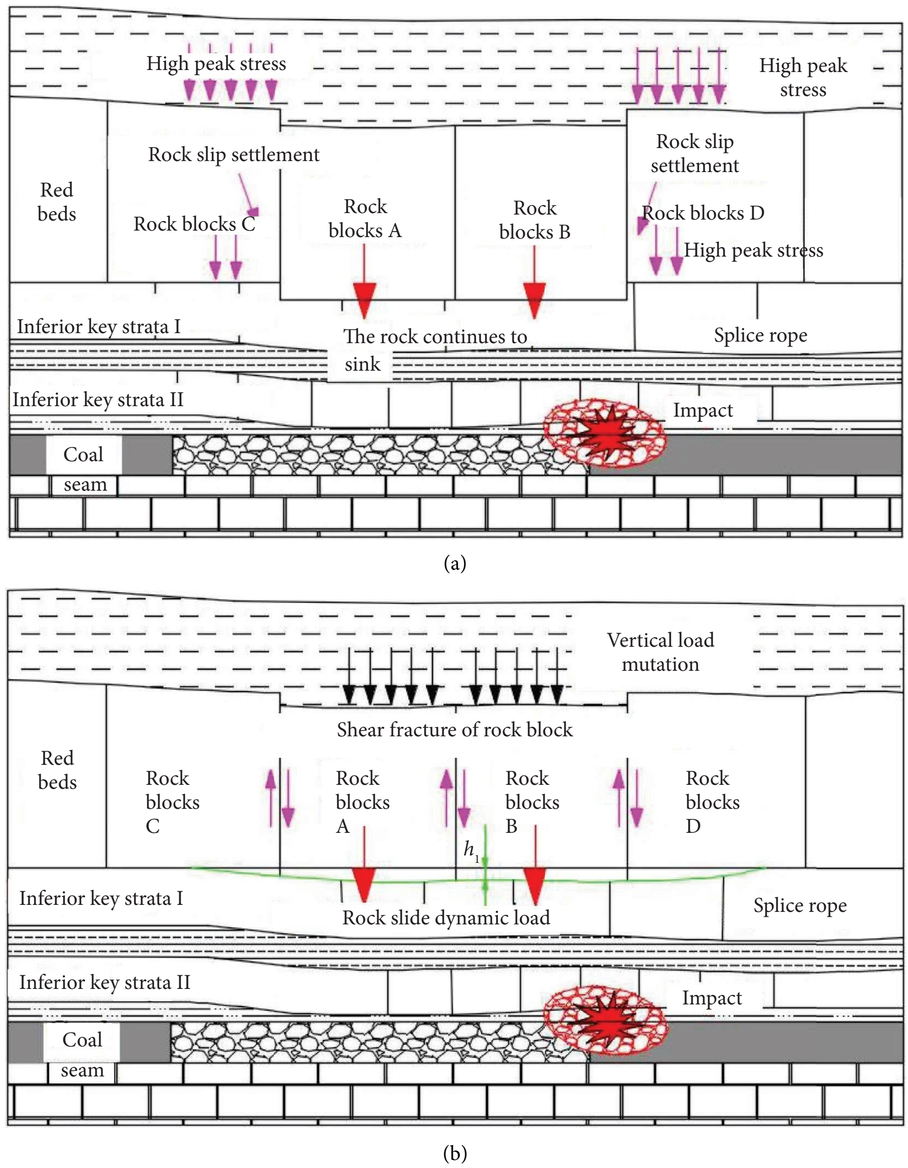

FIGURE 8: Rock burst-induced principle of hard rock coal mine earthquake. (a) Rock burst-induced principle of hard rock fracture. (b) Rock burst-induced principle of slip settlement.

the rock block C and rock block D slip caused the range of support points to be smaller and smaller. The rock blocks on both sides of rock block C and rock block D will be driven by certain slip. The strata movement line formed by the working face mining also expands outward.

In fact, it is not difficult to see that the two hard roof type coal mine earthquake rock burst-induced phenomenon is not independent and their relationships are mutual influence and promotion. The shear fracture of rock blocks A and rock blocks B sink. The vertical distance increases with rock blocks C and rock blocks D. It can intensify the tendency of rock blocks C and rock blocks D inclined sinking of rock mass. At the same time, the area of stress concentration was caused by rock blocks C and rock blocks D slip sinking will squeeze rock blocks A and rock blocks B and force them to sink further. They promote each other and strengthen the induction.

4.2. Rock Burst-Induced Principle of Fault-Type Coal Mine Earthquake. According to the coal mine earthquake law of the mining in fault zone and the motion characteristics of surrounding rock movement [30–32], the fault activation type, fault coal pillar type, and fault dislocation type rock burst were easily induced successively when working face passes through fault mining as shown in Figure 9. The following are described, respectively.

4.2.1. Rock Burst Mechanism Induced by Fault Activation. The faults were generally formed by horizontal stress extrusion. So, a lot of horizontal stress accumulated on both sides of section after the fault formed. The fault was severely activated by mining disturbance when the working face is close to the fault. The macroscopic fracture of coal-rock occurs in the roof and floor of coal seam near the fault. The original mechanical

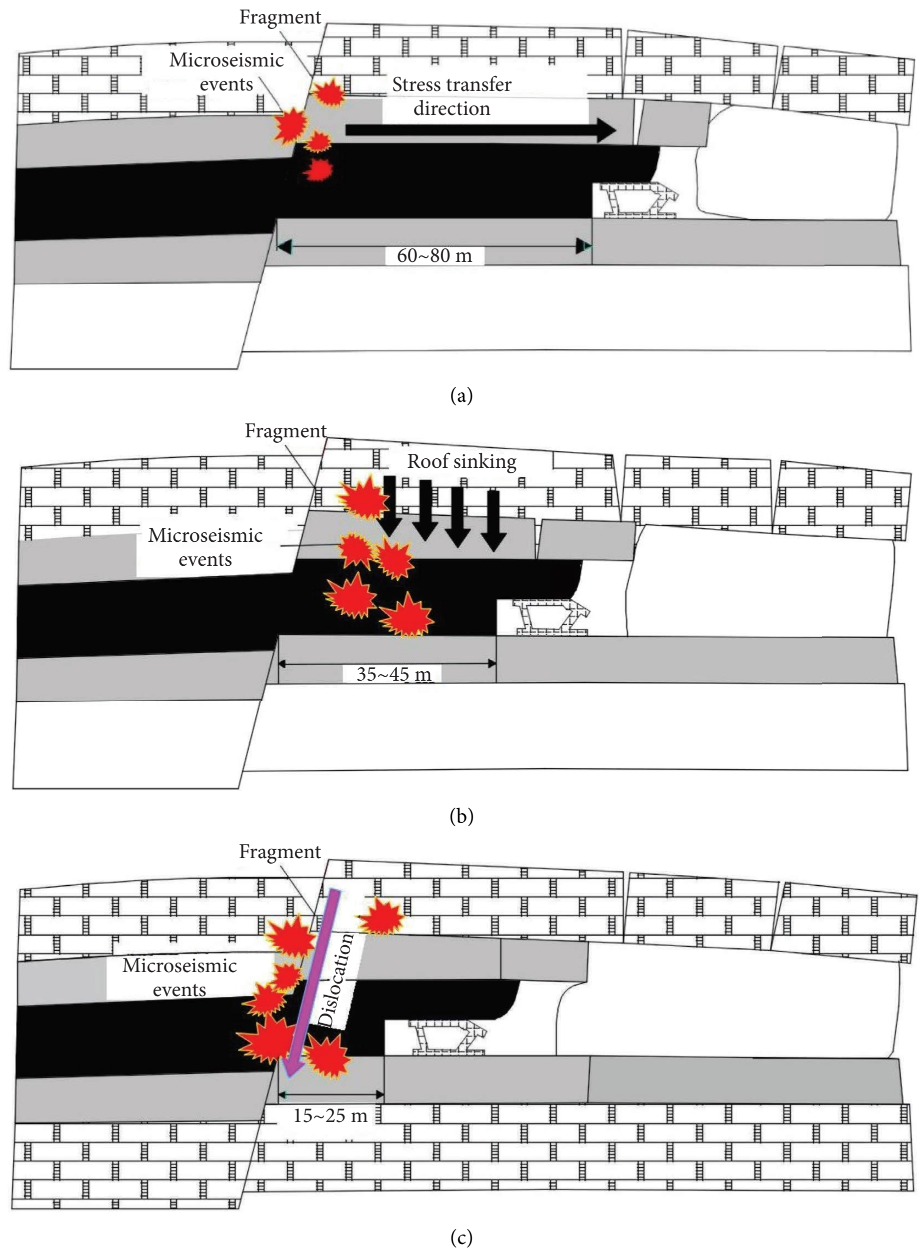

FIGURE 9: Rock burst-induced principle of fault coal mine earthquake. (a) Rock burst mechanism induced by fault activation. (b) Rock burst mechanism induced by fault coal pillar. (c) Rock burst mechanism induced by fault dislocation.

balance state was broken near the fault. The horizontal stress near the fault transfers to the coal rib. The appearance of impact was caused finally near the coal rib or roadway. The fault stress transfer process is shown in Figure 9(a).

4.2.2. Rock Burst Mechanism Induced by the Fault Coal Pillar. The continuous mining of coal seam and the coal rib is close to the fault. The fault cuts off coal seam roof to form small coal pillar between coal rib and section. The small coal pillar was difficult to support and yield failure under the influence of overburden weight load. At the same time, a large number of large energy microseismic events were formed. The formation of small fault coal pillars is easy to rock burst induced, as shown in Figure 9(b).

4.2.3. Rock Burst Mechanism Induced by Fault Dislocation. The faults have already experienced long-term activation when the working face mining was close to section. The "Lubricating" section was formed by fault mud gushing from section. In addition, the width of coal pillar at this time has reached a minimum. The small coal pillars have dislocated, released energy, and rock burst induced under the role of the dead weight of overlying strata, as shown in Figure 9(c).

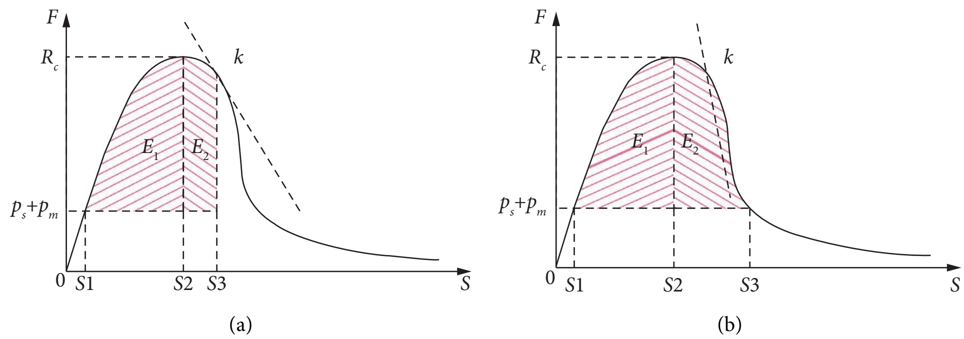

FIGURE 10: Stress-displacement relationship curve of rock burst induced by the coal mine earthquake. (a) Shock instability. (b) Static destruction.

4.3. Unified Rock Burst Mechanism due to Energy Difference Increases Suddenly. The occurrence law of coal mine earthquakes and spreading law of seismic energy were analyzed. The response characteristics of mine seismic activity, the basic principles of hard roof, and fault-type coal mine earthquake induced impulse. It is known that the large energy coal mine earthquake is induced by hard roof or fault slip dislocation. The nonlinear increased of energy near the adjacent coal rib. And the increase is the possibility of rock burst occurrence. The related research reference [33] shows that the occurrence of rock burst must also satisfy energy and stiffness conditions. The mechanism of rock burst induced by coal mine earthquakes was analyzed from the perspective of energy. First, the scalar superposition of coal mine earthquake energy and static load energy is formed in mining in the rock burst source area. Of course, the coal mine earthquake energy in the rock burst source area was determined by its propagation and dissipation characteristics. The greater shock energy was received by the rock burst source and the superposition effected stronger. The energy condition of impact instability was easier to reach. Similarly, the greater dynamic load was occurred by the coal mine earthquake. The superposition result of the static load vector was more easily formed by mining and can reach the limit strength of coal-rock destruction. The coal-rock mass enters a postpeak stage of its stress-strain curve after reaching its limit strength. The rock burst source area was destroyed. But it is not certain whether the impact damage or the stability damage will happen. Also, its determined need is according to the difference between energy superposition results and coal-rock failure energy consumption.

The load-displacement curves of the rock under shock and static failure are shown in Figure 10. F is the load, MPa. S is the displacement, m. P_s and P_m are the mine vibration load and mining static load, MPa. E_1 and E_2 are energy consumed by coal accumulation and destruction, J. The coal mine earthquake makes the stress of coal-rock reach the postpeak point S_3 in an instant, as shown in Figure 10(a). This greatly reduces the energy consumed by coal-rock destruction (E_2 area in the figure). So, the energy difference ΔE ($\Delta E = E_1 - E_2$) between coal accumulation and destruction increases greatly. The occurrence possible of rock bursts was increased. The coal mine earthquake energy was greater and the rock burst strength was stronger. At the same time, the disturbance effect of the coal mine earthquake acts on the rock burst source region. And the unloading stiffness k of shock source region decreases. The strong rock burst occurs when $k + F' \ (S) < 0$ ($F \ (S)$) is the expression of load-displacement curve.

In another case, the coal was destroyed under the disturbance of coal mine earthquake. But there was no rock burst occur. This situation usually occurs when the lithology of the rock burst source area is soft and the impact tendency is low, as shown in Figure 10(b). The disturbance of the coal mine earthquake can also increase the difference energy ΔE. But the unloading stiffness of rock burst source region cannot satisfy the $k + F' \ (S) < 0$. The energy of rock burst source region was slow released. This results in the static energy release failure rather than the violent shock accident. The comparison is shown in Figures 10(a) and 10(b). The impact energy index $K_E = E_1/E_2$ (Figure 10(a)) under the seismic disturbance is greater than the impact energy index of static failure (Figure 10(b)).

So, the criterion of rock burst instability under the seismic disturbance was expressed as

$$\begin{cases} E_s + E_m \geq \int_{s_1}^{s_2} \left[F(s) - (p_s + p_m)\right] \mathrm{d}s, \\ k + F'(s) \leq 0. \end{cases} \quad (2)$$

In the formula, E_m is the mining static load energy, J. E_s is the load energy of coal mine earthquake, J. $F \ (s)$ is the load-displacement curve expression. k is the unloading stiffness. P_s and P_m represent the coal mine earthquake load and mining static load, MPa.

5. Conclusions

In this study, the microseismic data have been widely used to study the law of coal mine earthquakes activity. On this basis, the mechanism of rock bursts induced by different types of coal mine earthquakes is studied based on theoretical methods. Finally, the unified mechanism of rock bursts induced by coal mine earthquakes is analyzed from the perspective of rock mechanics. The main research conclusions are as follows:

(1) The law of coal mine earthquakes under the condition of hard roof and fault was analyzed. And the hard roof movement of working face was the key factor leading to a strong coal mine earthquake. The microseismic energy increases sharply and decreases sharply when mining in the fault area. The low-energy microseismic event stores energy for the strong coal mine earthquake. The amplitude and frequency of support resistance increase before and after the strong coal mine earthquake. The periodic characteristics of the coal mine earthquake in 43_{upper} 13 working face of the Dongtan coal mine shows that there are small periods of 50 m within large periods of 100 m.

(2) The description formula has fine adjusted previous seismic energy propagation dissipation characteristics. The description method of considering the hypocenter scale seismic energy propagation dissipation characteristics was proposed. The moment of field coal mine earthquake was transient captured by the coal-rock stress meter, roof separation meter, and bolt stress meter. It considered that the multi-parameter transient capture of a strong coal mine earthquake dynamic response can roughly determine the hypocenter location and evaluate the disaster degree.

(3) The two principles of rock bursts induced by hard rock and the three principles of rock bursts induced by fault were described. The principle of rock burst induced by hard rock was divided into hard rock shear fracture rock burst induced and slip settlement rock burst induced. The rock bursts induced by fault include rock burst induced by fault activation, rock burst induced by fault coal pillar, and rock burst induced by fault dislocation. The unified rock burst mechanism induced different types of coal mine earthquake and the difference energy between the superposition energy of rock burst source region and energy consumed by coal-rock instability increases suddenly under the action of coal mine earthquakes. Meanwhile, the violent rock burst accident occurs when the stiffness condition is satisfied.

Data Availability

The data used to support the findings of this study are available from the corresponding author upon request.

Conflicts of Interest

The authors declare that there are no conflicts of interest.

Acknowledgments

This study was supported by the Natural Science Foundation of Inner Mongolia Autonomous Region (no. 2019LH05005) and the Innovation Foundation of Inner Mongolia University of Science and Technology (no. 2019QDL-B32).

References

[1] L. M. Dou and X. Q. He, *Theory and Technology of Rock Burst Prevention*, University of Mining and Technology Press, Xuzhou: China, 2001.

[2] Q. X. Qi, S. B. Chen, H. X. Wang, D. B. Mao, and Y. X. Wang, "Study on the relations among coal bump, rockburst and mining tremor with numerical simulation," *Chinese Journal of Rock Mechanics and Engineering*, vol. 22, no. 11, pp. 1852–1858, 2003.

[3] C. P. Lu, L. M. Dou, A. Y. Cao, X. R. Wu, and Z. H. Li, "Research on microseismic activity rules in deep high-stress concentration district," *Chinese Journal of Rock Mechanics and Engineering*, vol. 27, no. 11, pp. 2303–2308, 2008.

[4] Z. B. Tang, "Research on law of mining earthquakes in a coal mine of Yanzhou," *Chinese Journal of Rock Mechanics and Engineering*, vol. 30, no. S2, pp. 4143–4152, 2011.

[5] A. Y. Cao and L. M. Dou, "Analysis of focal mechanism caused by rupture of stope roof," *Chinese Journal of Rock Mechanics and Engineering*, vol. 27, no. S2, pp. 2833–2839, 2008.

[6] Y. Yu, D. X. Geng, L. h. Tong, X. S. Zhao, X. H. Diao, and L. H. Huang, "Time fractal behavior of microseismic events for different intensities of immediate rock bursts," *International Journal of Geomechanics*, vol. 18, no. 7, Article ID 06018016, 2018.

[7] G. Q. Chen, T. B. Li, G. F. Zhang, H. Y. Yin, and H. Zhang, "Temperature effect of rock burst for hard rock in deep-buried tunnel," *Natural Hazards*, vol. 72, no. 2, pp. 915–926, 2014.

[8] K. Zhao, K. Z. Zhang, and S. L. Wang, "Study on movement law of ultra thick overlying strata broken and coal mine earthquakes," *Coal Science and Technology*, vol. 44, no. 2, pp. 118–122, 2016.

[9] S. L. Wang, G. L. Zhu, K. Z. Zhang, and L. Yang, "Study on characteristics of mining earthquake in multicoal seam mining under thick and hard strata in high position," *Shock and Vibration*, vol. 2021, Article ID 6675089, 17 pages, 2021.

[10] L. Pengfei, B. Xinyang, L. Gang, and C. Xuehua, "Research on fault activation law in deep mining face and mechanism of rockburst induced by fault activation," *Advances in Civil Engineering*, vol. 2020, Article ID 8854467, 1–3 pages, 2020.

[11] H. Zhang, Z. H. Ouyang, T. Li et al., "An investigation into the mechanism of rock bursts in mines for tunnel-cut isolated areas with multiple stress fields," *Frontiers of Earth Science*, vol. 9, Article ID 8098392, 2022.

[12] A. Y. Cao, L. M. Dou, H. L. Wang, and A. King, "Experimental research on seismic wave transmission and attenuation associated with underground longwall coal mining," *Journal of mining and safety engineering*, vol. 28, no. 4, pp. 530–535, 2011.

[13] X. X. Bai, A. Cao, W. Cai et al., "Rock burst mechanism induced by stress anomaly in roof thickness variation zone: a case study," *Geomatics, Natural Hazards and Risk*, vol. 13, no. 1, pp. 1805–1830, 2022.

[14] P. F. Lyu, X. H. Chen, G. B. Chen, and L. Qiu, "Experimental study on dynamic mechanical responses of coal specimens under the combined dynamic-static loading," *Arabian Journal of Geosciences*, vol. 13, no. 18, 935 pages, 2020.

[15] H. W. Wang, Y. D. Jiang, C. Jiang, J. H. Di, and Y. Y. Liu, "Characteristics of overlying strata movement in double fault area under the dynamic pressure," *Journal of Mining & Safety Engineering*, vol. 36, no. 3, pp. 513–518, 2019.

[16] S. M. Yang, N. B. Zhang, J. Liu, and S. K. Zhao, “Research on mechanism of fault rock burst,” *Coal Science and Technology*, vol. 42, no. 10, pp. 6–9+27, 2014.
[17] S. M. Yang, X. Y. Sun, and S. N. Wang, “Study on parameters of bolt-mesh-cable combined support technology in large cross-section roadway,” *Nonferrous Metals*, vol. 63, no. 2, pp. 230–232, 2011.
[18] S. G. Li, J. G. Lv, Y. D. Jiang, and W. Z. Jiang, “Coal bump inducing rule by dip angles of thrust fault,” *Journal of mining and safety engineering*, vol. 31, no. 6, pp. 869–875, 2014.
[19] W. Wang, B. S. Jia, Y. Qi, and S. G. Li, “Experimental research on optimization of water resources treatment conditions for high turbidity mines,” *Non-metallic Mines*, vol. 44, no. 1, pp. 81–84, 2019.
[20] J. Q. Jiang, Q. L. Wu, and H. Qu, “Evolutionary characteristics of mining stress near the hard-thick overburden normal faults,” *Journal of mining and safety engineering*, vol. 31, no. 6, pp. 881–887, 2014.
[21] J. Q. Jiang, P. P. Zhang, G. P. Qin, and B. Xu, “Analysis of destabilized fracture and microseismic activity of high-located main key strata,” *Rock and Soil Mechanics*, vol. 36, no. 12, pp. 3567–3575, 2015.
[22] L. Pengfei and C. Xuekai, “Mechanism of vibration energy action on dynamic instability of shock-type rockburst carrier system,” *Shock and Vibration*, vol. 2020, Article ID 6663269, 10 pages, 2020.
[23] K. Y. Zhou, L. M. Dou, X. W. Li et al., “Coal burst and mining-induced stress evolution in a deep isolated main entry area - a case study,” *Engineering Failure Analysis*, vol. 137, Article ID 106289, 2022.
[24] L. Pengfei, L. Jiabin, W. Eryu, and C. Xuehua, “The mechanical criterion of activation and instability of normal fault induced by the movement of key stratum and its disaster-causing mechanism of rockburst in the hanging wall mining,” *Advances in Civil Engineering*, vol. 2021, Article ID 6618957, 11 pages, 2021.
[25] S. T. Zhu, D. C. Ge, F. X. Jiang et al., “Rock burst mechanism under coupling action of working face square and regional tectonic stress,” *Shock and Vibration*, vol. 2021, Article ID 5538179, 11 pages, 2021.
[26] T. Wang, S. You, F. Pei, and X. P. Bai, “Instability mechanism and control technology of coal pillar bumps under hard roof,” *Journal of Mining & Safety Engineering*, vol. 34, no. 1, pp. 54–59+66, 2017.
[27] L. L. Cao, B. W. Luo, H. L. Gao, M. Miao, T. Wang, and Y. Deng, “Structure induced wide range wettability: controlled surface of micro-nano/nano structured copper films for enhanced interface,” *Journal of Materials Science & Technology*, vol. 84, pp. 147–158, 2021.
[28] Z. L. Mu, L. M. Dou, G. W. Zhang, S. B. Zhang, Z. H. Li, and J. Zhang, “Study of prevention methods of rock burst disaster caused by hard rock roof,” *Journal of China University of Mining & Technology*, vol. 35, no. 6, pp. 737–741, 2006.
[29] G. J. Liu, M. Karakus, and Z. L. Mu, “Propagation and attenuation characteristics of rockburst-induced shock waves in coal-rock medium,” *Arabian Journal of Geosciences*, vol. 12, no. 4, 113 pages, 2019.
[30] L. B. Song, Q. Jiang, Z. Zhong et al., “Technical path of model reconstruction and shear wear analysis for natural joint based on 3D scanning technology,” *Measurement*, vol. 188, Article ID 110584, 2022.
[31] L. B. Song, G. Wang, X. K. Wang et al., “The influence of joint inclination and opening width on fracture characteristics of granite under triaxial compression,” *International Journal of Geomechanics*, vol. 22, no. 5, Article ID 04022031, 2022.
[32] Y. Luo, G. Wang, X. P. Li et al., “Analysis of energy dissipation and crack evolution law of sandstone under impact load,” *International Journal of Rock Mechanics and Mining Sciences*, vol. 132, Article ID 104359, 2020.
[33] S. P. Singh, “Burst energy release index,” *Rock Mechanics and Rock Engineering*, vol. 21, no. 2, pp. 149–155, 1988.